Eur Biophys J (2010) 39:1343–1350
DOI 10.1007/s00249-010-0587-x

ORIGINAL PAPER

Interaction of hnRNP A1 with telomere DNA G-quadruplex structures studied at the single molecule level

A. C. Krüger · M. K. Raarup · M. M. Nielsen · M. Kristensen · F. Besenbacher · J. Kjems · V. Birkedal

Received: 27 July 2009 / Revised: 7 December 2009 / Accepted: 12 February 2010 / Published online: 8 March 2010

Abstract G-rich telomeric DNA sequences can form G-quadruplex structures. The heterogeneous nuclear ribonucleoprotein A1 (hnRNP A1) and a shortened derivative (UP1) are active in telomere length regulation, and it has been reported that UP1 can unwind G-quadruplex structures. Here, we investigate the interaction of hnRNP A1 with G-quadruplex DNA structures containing the human telomere repeat (TTAGGG) by gel retardation assays, ensemble fluorescence energy transfer (FRET) spectroscopy, and single molecule FRET microscopy. Our biochemical experiments show that hnRNP A1 binds well to the G-quadruplex telomeric DNA. Ensemble and single molecule FRET measurements provide further insight into molecular conformation: the telomeric DNA overhang is found to be in a folded state in the absence of hnRNP A1 and to remain predominantly in a compact state when complexed with hnRNP A1. This finding is in contrast to the previously reported crystal structures of UP1-telomere DNA complexes where the DNA oligo within the protein-DNA complex is in a fully open conformation.

Keywords Telomere DNA · DNA protein interaction · Single molecule microscopy · Fluorescence resonance energy transfer

Electronic supplementary material The online version of this article (doi:10.1007/s00249-010-0587-x) contains supplementary material, which is available to authorized users.

A. C. Krüger · M. K. Raarup · M. Kristensen · F. Besenbacher · J. Kjems · V. Birkedal (✉)
Interdisciplinary Nanoscience Center (iNANO), Aarhus University, Ny Munkegade 118, Building 1521, 8000 Århus C, Denmark
e-mail: vicb@inano.au.dk

A. C. Krüger · M. K. Raarup · M. Kristensen · F. Besenbacher
Department of Physics and Astronomy, Aarhus University, Ny Munkegade 120, 8000 Århus C, Denmark

M. M. Nielsen · J. Kjems
Department of Molecular Biology, Aarhus University, C.F. Møllers Allé 3, 8000 Århus C, Denmark

Present Address:
M. K. Raarup
Stereology and EM Research Lab. c/o Institute of Anatomy, University of Aarhus, Wilhelm Meyers Allé 3, Building 1234, 8000 Århus C, Denmark

Introduction

Telomeres are repeated sequences found at the end of linear chromosomes where they ensure complete replication and protect the chromosome ends from being recognized as damaged sites in need of repair (Blackburn 2001). Telomeres are thus essential for genome integrity and appear to play an important role in cellular aging and cancer. Telomeres are double-stranded but terminate with a single-stranded G-rich overhang at the 3′ end terminus. The telomeric repeat sequence for vertebrates is TTAGGG, which has been shown to form unusual structures in vitro called G-quadruplexes. These structures have been found to block telomerase elongation (Zahler et al. 1991) and are thus considered interesting targets for the design of new therapeutic and anticancer drugs. Moreover, there are indications that G-quadruplexes exist in vivo and that they may play a role in telomere capping (Paeschke et al. 2005).

Telomeres have been shown to interact with a number of proteins. One of them is the heterogeneous nuclear ribonucleoprotein A1 (hnRNP A1), which is a 319 amino acid protein abundant in the eukaryotic nucleus, and which is also known to play a role in mRNA processing. hnRNP A1 and its shortened derivative UP1 co-localize with telomeres

in vivo, and, together with other proteins of the same family, they interact with single-stranded telomeric sequences (Ishikawa et al. 1993; Ding et al. 1999; Dallaire et al. 2000; Zhang et al. 2006), as well as with telomerase (Fiset and Chabot 2001; Ford et al. 2002). hnRNP A1/UP1 has also been found to influence telomerase activity (Dallaire et al. 2000; Fiset and Chabot 2001; Zhang et al. 2006), and Zhang et al. suggested that hnRNP A1 can stimulate telomere activity through unwinding of G-quadruplex structures (Zhang et al. 2006). Several other studies report that UP1 binding induces an unfolding of the G-quadruplex (Fukuda et al. 2002; Myers et al. 2003). In in vivo studies it was observed that short telomeres produced in certain hnRNP A1–deficient mouse cells are elongated after re-establishment of hnRNP A1 expression (LaBranche et al. 1998), and that the expression level of hnRNP A1 is higher in certain human cancer cells than in normal tissue (Patry et al. 2003). Although the exact mechanism of the interaction is still under debate, it is generally agreed that hnRNPA1 plays an important role in regulating telomere length.

Here, we investigate the interaction of the hnRNP A1 protein with a telomere DNA structure folded into a G-quadruplex using gel shift and fluorescence resonance energy transfer (FRET) assays. By studying the FRET signal from single DNA molecules the different conformations within a heterogeneous population can be analyzed. FRET can occur between two fluorescent probes (donor and acceptor) attached to the molecule of interest. The efficiency depends on the inverse sixth power of the donor–acceptor distance and hence is very sensitive in detecting changes in conformation on the 3–8 nm scale (Lakowicz 2006). This is the regime relevant for monitoring several biological processes, including the unfolding of the G-quadruplex structure. We find that hnRNP A1 binding modifies the FRET efficiency distribution of the folded G-quadruplex population, with a significant number of the molecules switching to a low FRET efficiency conformation following hnRNP A1 incubation. Low FRET efficiencies imply that the DNA molecules are in relatively open conformations. On the other hand, gel shift assays under the same binding conditions show that hnRNP A1 binding is more effective than observed in our FRET studies. This finding implies that only part of telomere DNA in the hnRNP A1–bound telomere complex is in an open conformation.

Experimental procedures

Materials

Labeled and gel purified DNA oligonucleotides were purchased from IBA Germany. Constructs include the following: **I** Cy5-GGG $(TTAGGG)_3$ AGA GGT AAA AGG ATA ATG GCC ACG GTG CGG ACG GC, **II** biotin-GCC GTC CGC ACC GTG GCC ATT ATC CTT XTA CCT CT (X represents Cy3 NHS labeled to a T base), **III** AGA GGT AAA AGG ATA ATG GCC ACG GTG CGG ACG GC, **IV** GCA GGC GTG GCA CCG GTA ATA GGA TXA GGG TTA GGG TTA GGG TTA GGG TTA GGG-CY5, **V** TAA CCC TAA TCC TAT TAC CGG TGC CAC GCC TGC-biotin, and **VI** GCA GGC GTG GCA CCG GTA ATA GGA TTA GGG TTA. DNA oligonucleotides equivalent to I, II, IV, and V were also purchased unlabeled.

Concentrations of DNA oligos were verified by absorption spectroscopy, and hybridization was performed by incubation in 20 mM HEPES-KOH (pH 7.6) and 150 mM KCl for 5 min at 90°C followed by 1 h

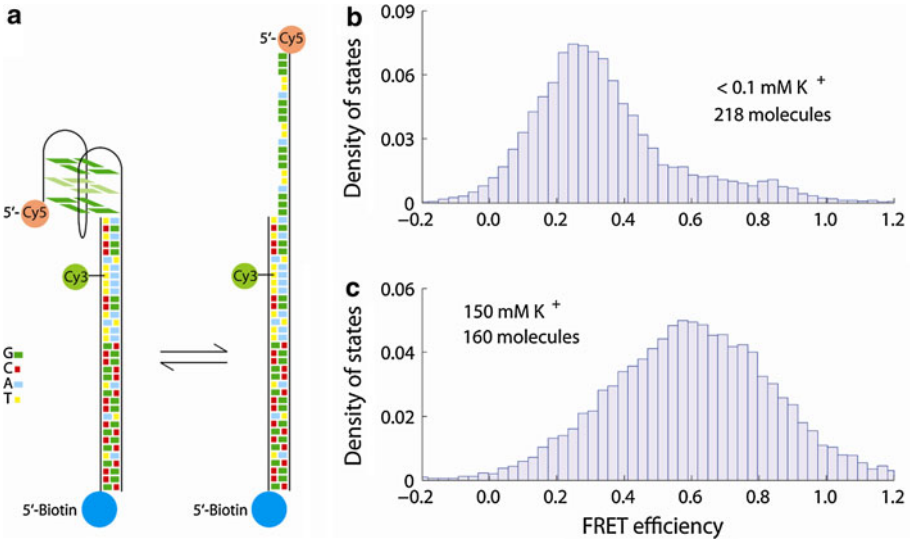

Fig. 1 **a** Schematic representation of the DNA construct Tel_I_II in a folded (*left*) and unfolded (*right*) conformation. **b** and **c** Single molecule FRET efficiency histograms (density of states as a function of FRET efficiency based on single molecule FRET efficiency time traces) for the construct Tel_I_II. The DNA was incubated in 20 mM Tris-HCl buffer, pH 7.5, and **a** <0.1 mM KCl and **b** 150 mM KCl

equilibration to room temperature. Hybridization of **I** and **II** yields the construct Tel_I_II shown schematically in Fig. 1, where the telomere repeat sequence is positioned at a protruding 5′ end. Similarly, **IV** and **V** yield a construct (Tel_IV_V) where the telomere repeat sequence is positioned at a protruding 3′ end. Strands **II** and **III** and strands **V** and **VI** were also hybridized for control purposes yielding a blunt-ended DNA without telomeric overhang.

The hnRNPA1 protein was expressed as previously described (Tange et al. 2001).

Electrophoretic mobility shift assay

Probes for electrophoretic mobility shift assay were prepared by radioactive 5′ end-labeling of oligos II and V using T4 polynucleotide kinase (New England Biolabs). The labeled oligos were purified on G-50 spin columns and subsequently annealed to complementary oligos to produce test constructs with 5′-overhang, 3′-overhang, or blunt end.

A 5 nM sample of annealed probe was incubated with or without 500 nM hnRNP A1 protein in binding buffer [10 mM HEPES (pH 7.7), 150 mM KCl, 0.2 mM EDTA] for 30 min at room temperature. Samples were resolved on a 6% native polyacrylamide gel containing 50 mM Tris-borate (pH 7.2) and 100 mM KCl.

Protein binding in the electrophoretic-mobility shift assay was quantified by scanning the gel with a Molecular Imager FX from Bio-Rad. Band intensities were integrated from the image file with appropriate background subtraction using the Quantity One software package. No saturation effects were observed in the image file. The fraction of protein binding was calculated as the intensity of DNA-protein complex in the lowest DNA-protein complex band divided by the sum intensity of all bands in the lane.

Ensemble FRET spectroscopy

Ensemble FRET spectroscopy measurements were carried out on a Fluoromax 3 fluorimeter (Horiba Yobin-Yvon) at 22 and 37°C at a DNA concentration of 50 nM and at different hnRNP A1 concentrations ranging from 0 to 1 μM in FRET buffer [20 mM HEPES-KOH (pH 7.6) with 150 mM KCl—leading to 163 mM K^+—and 0.2 mM Titriplex III EDTA]. FRET efficiencies were calculated by the Ratio A method (Clegg 1992). Steady state polarization anisotropy was also determined.

Single molecule FRET microscopy

The experimental setup for single-molecule FRET microscopy is based on a wide-field optical microscope (Cognet et al. 2000). The sample was mounted on an inverted microscope (Axiovert 200, Zeiss) equipped with a high numerical aperture objective (Plan Apochromat ×100, oil immersion, NA 1.4, Zeiss). Fluorophore excitation was provided by the 514 nm line of an Ar^+-ion laser (Beamlok 2060, Spectra Physics) and the 630 nm output of a dye laser (CR-599-12, Coherent). The light was pulsed by an Acousto-Optic Tuneable Filter (AA.AOTF.nC, A-A Opto-Electronic) to provide alternating donor-acceptor excitation, with the acceptor being directly excited every 51st image. Donor excitation is in principle sufficient to detect FRET, but direct acceptor excitation provides additional control, similarly to the ALEX scheme (Lee et al. 2005a). The laser light was brought to the microscope by a single-mode polarization preserving optical fiber (OZ Optics) filtered through an aperture, circularly polarized by a $\lambda/4$ plate and focused onto the back focal plane of the objective by a 40 cm lens. Illumination intensities were 1.4 kW/cm^2 for the 514 nm light and 0.4 kW/cm^2 for the 630 nm light. The illumination time was 50 ms per image, and images were taken at 6.2 Hz. Measurements with half of the illumination intensities were also taken and yielded similar results. Donor and acceptor fluorescence signals collected by the objective were passed through a dichroic mirror and an emission filter (Chroma), spatially split with a custom designed dichroic wedge mirror (Chroma) and imaged with a 12.5 cm achromatic lens onto a peltier cooled back illuminated CCD camera (MicroMax 512BFT, Roper Scientific).

The DNA molecules (~10 pM in 100 μL) were tethered to a glass coverslip through BSA-biotin streptavidin interaction, which enabled us to follow the behavior of single molecules in time (Ha 2001). Therefore, before adding DNA, the coverslip was incubated for 5 min each: first with 0.1 g/L BSA-biotin (Sigma-Aldrich, A8549), then with 0.1 g/L streptavidin (Molecular Probes, S-888). Unless otherwise specified, all experiments were performed in 20 mM HEPES-KOH buffer (pH 7.6) with 150 mM KCl—yielding 163 mM K^+ in total—and 0.2 mM Titriplex III EDTA (Merck, K33219418 422) in the presence or absence of 500 nM of hnRNP A1. Samples were prepared in solution and subsequently attached to the coverslip surface for single molecule measurements. The buffer also contained an anti-bleaching cocktail composed of 4.5 mg/mL glucose (Sigma G7528), 0.92 mg/mL glucose oxidase (Sigma G2133), 20 mg/mL DTT (Sigma 457779-5G), and 0.04 mg/mL catalase (Roche 0106810) (Yildiz et al. 2003).

Data analysis was performed by a software package written in MATLAB (MathWorks), with initial peak fitting using a Gaussian correlation filter (Schmidt et al. 1995), where fluorescence peaks in donor and acceptor channels were correlated to find co-localized donor-acceptor fluorescence spots. Background signals were evaluated and subtracted from the fluorescent signals. FRET efficiencies

were calculated from the donor and acceptor fluorescence intensities as $E = I_A/(I_A + \gamma I_D)$, where I_A and I_D are the measured fluorescence of acceptor and donor, respectively, after background and donor leakage correction (Roy et al. 2008), and $\gamma = \frac{\eta_A \varphi_A}{\eta_D \varphi_D}$ is a correction factor that accounts for the difference in detection efficiencies η_A and η_D and quantum yields φ_A and φ_D for the two fluorophores. For our setup and with the studied constructs, we found $\gamma \sim 1.4$. The data were filtered by a series of threshold criteria, and partially labeled molecules were removed. Fluorescence time traces [examples shown in Figure S1 of the Electronic Supplementary Material (ESM)] were finally inspected to check that all pairs of donor acceptor peaks were displaying FRET characteristics and to remove the parts of the data series where donor or acceptor had been bleached. This procedure allowed us to increase the range of the FRET efficiency measurement as we were able to efficiently suppress the FRET efficiency peak that usually appears in histograms at $E = 0$ and that is due to bleached acceptors (Lee et al. 2005a).

Experimental results

A double-stranded DNA construct (Tel_I_II) with a protruding single-stranded telomeric 5′ overhang repeat sequence was constructed (Fig. 1a). To monitor folding and unfolding of the single-stranded DNA region, Cy3 (donor) and Cy5 (acceptor) fluorophores were positioned as shown in Fig. 1a (see also Fig. 4a). Measuring donor and acceptor fluorescence signals allowed us to assess the relative distance between the fluorophores and hence the conformational state of the DNA. To test the DNA construct, single molecule FRET was recorded at low (<0.1 mM KCl) and high (150 mM KCl) K^+ concentrations; the latter is known to efficiently stimulate G-quadruplex structure formation (Kankia and Marky 2001; Ambrus et al. 2006). The data from single molecule FRET efficiency time traces for Tel_I_II at low and high KCl concentration are represented in FRET efficiency histograms in Fig. 1b and c, respectively. At low K^+ concentration, the FRET efficiency histogram shows a peak at around 0.25, while at high K^+ concentration the FRET efficiency distribution is centered at a higher FRET value of ~0.6. These measurements are consistent with previous single molecule studies (Ying et al. 2003; Lee et al. 2005b) showing that K^+ ions stabilize the G-quadruplex structure and bring the donor and acceptor fluorophores into close proximity with each other. The width of the observed high FRET efficiency peak suggests that several conformations of the G-quadruplex may co-exist including the parallel, anti-parallel, or hybrid conformations described previously (Li et al. 2005; Luu et al. 2006; Xu et al. 2006). At low salt concentration, the FRET efficiency peak at around 0.25 (Fig. 1b) can be interpreted as the unfolded state, where the donor and acceptor are farther away from each other (Fig. 1a). Similar observations were obtained for the Tel_IV_V construct that contains a 3′ end overhang (data not shown; Fig. 3d). However, in this case, FRET efficiency peaks are narrower for the sample Tel_IV_V, which is largely due to the fact that measurements for Tel_IV_V are less noisy than for Tel_I_II; examples of single molecule fluorescence time traces for both DNA constructs are shown in Fig. S1of the ESM.

Next, the interaction between the hnRNP A1 protein and telomere constructs was investigated in a gel retardation assay under high salt conditions, which favor formation of G-quadruplexes (Fig. 2 and Fig. S2 in the ESM). The hnRNP A1 protein interacts both with Tel_I_II, which contains a 5′ overhang, and with Tel_IV_V, which contains a 3′ overhang, with a preference for the latter (45 vs. 80% complex formation at 500 nM hnRNPA1, respectively; Fig. 2, lanes 1, 2 and 5, 6). Some minor DNA-protein complex bands were observed above a major complex, which suggests that multiple hnRNP A1 molecules may bind with lower affinity. Binding of hnRNPA1 to constructs without protruding single-stranded DNA was negligible (Fig. 2, lanes 3, 4 and 7, 8). Measurements were also performed with Tel_I_II and Tel_IV_V constructs that did not contain fluorescent labels, and Cy3- or Cy5-labels did not appear to inhibit protein binding significantly (Fig. S2 in the ESM).

The effect of hnRNP A1 on the telomere conformation was further investigated by FRET spectroscopy and microscopy. Ensemble measurements show that the average FRET efficiency decreases by ~4% for Tel_IV_V with 3′ overhang and ~6% for Tel_I_II with 5′ overhang when 500 nM hnRNP A1 protein is added to the solution (see Fig. S3 in the ESM). The decrease is observed already after 5 min of incubation without any further decrease after 30 min (result not shown). Importantly, the presence of the protein did not significantly alter the steady state polarization anisotropy or change the quantum yield of the fluorophores. Thus, the observed change in the FRET efficiency is most likely due to a change in conformation and not to a change in the fluorescent properties of the dyes. It is also sensitive to temperature as an increase in temperature to 37°C led to a twofold increase in the differential FRET efficiency signal with and without protein (see Table S4 in the ESM).

Single molecule FRET efficiency time traces were measured at room temperature for Tel_I_II and Tel_IV_V, and the results are presented in FRET efficiency histograms in the absence (Fig. 3a, d) and presence (Fig. 3b, f) of the hnRNP A1 protein. A difference plot of the FRET efficiency histograms is shown in Fig. 3c, f. The shift towards

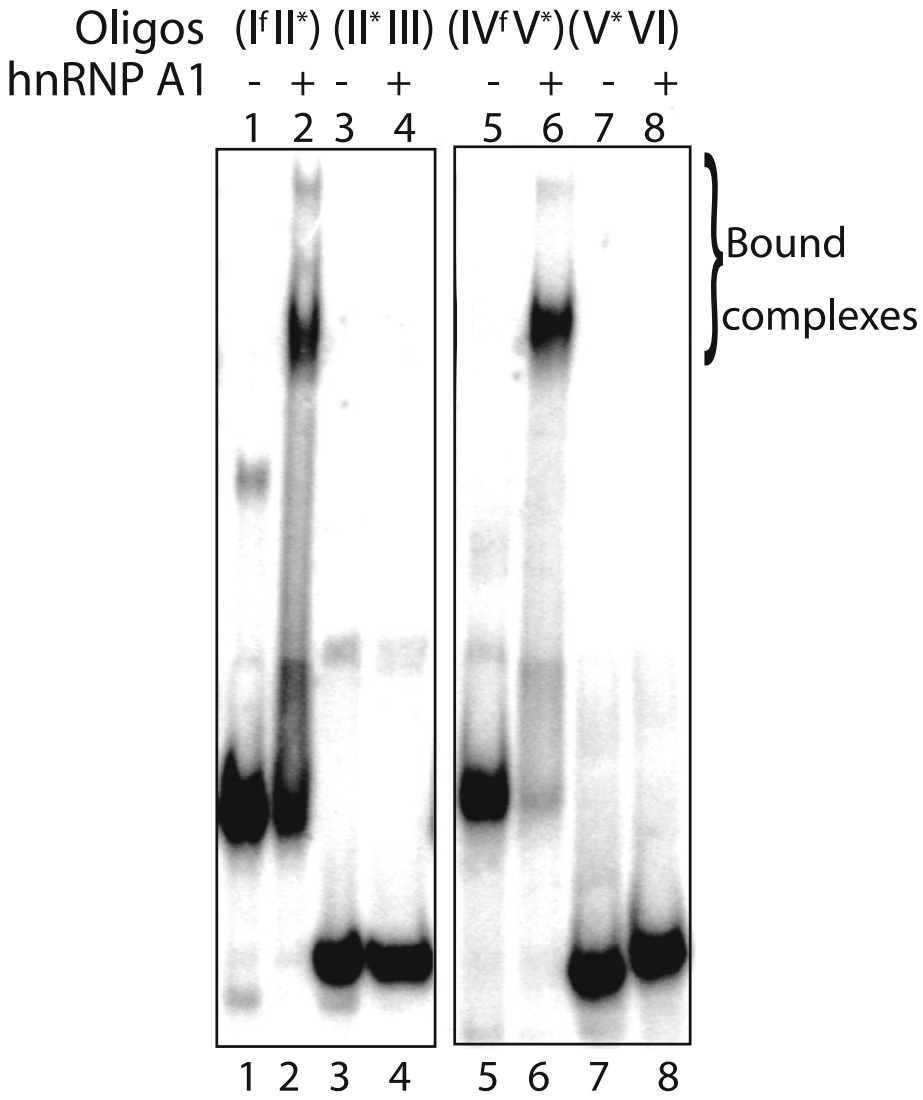

Fig. 2 Gel mobility shift assay in the absence and presence of 500 nM hnRNP A1. *Lanes 1, 2*: Tel_I_II where strand I is Cy5 labeled, *lanes 3, 4*: complex II-III, *lane 5, 6*: Tel_IV_V where strand IV is labeled both with Cy3 and Cy5, *lanes 7, 8*: complex V-VI. Samples on the figure are only referred to by their DNA strand numbers; an *asterisk* marks the oligo that was radioactively labeled at the 5′ end. *f* marks the presence of fluorophores

low FRET efficiency states in the presence of hnRNP A1 indicates that binding of hnRNP A1 partially influences the conformation of the G-quadruplexes (Fig. 3). Based on a comparison of the population in Fig. 3c, a with Fig. 3f, d, respectively, we estimate that the low FRET efficiency states below 0.5 show ~13% increase for Tel_I_II in the presence of protein, while Tel_IV_V shows ~5% increase. Unspecific protein surface adsorption can occur in our single molecule experiments as revealed in previous studies (Heyes et al. 2004). This effect may reduce the protein concentration in solution and perturb the formation of the DNA-protein complex. To investigate the influence of surface effects, we have carefully compared the single molecule data with ensemble FRET spectroscopy measurements, where we are mostly probing molecules that are freely diffusing in solution. We find that the differences between average FRET efficiencies in the absence of and in the presence of protein, respectively, are similar for the single molecule and ensemble FRET measurements. The single molecule measurements result in an average FRET efficiency change of 5 and 2% for Tel_I_II and Tel_IV_V, respectively. Although the average change in FRET efficiency is only of a few percent, hnRNP A1 induces a shift in the FRET value distribution reflecting an increase in donor–acceptor distance upon protein binding.

The presence of bands between the unbound and protein-bound complex in the gel assay of Fig. 2 may indicate the presence of oligo dimers that may form G-quadruplexes (Wang and Patel 1993). We analyzed the single molecule FRET data shown in Fig. 3 for contribution from any potential oligo dimers by comparing the intensity of individual single molecule measurements to what we expect if only one molecule is present. We find that, for both DNA constructs, several of our measurements correspond to two molecules being detected at the same time. Tel_IV_V shows the largest fraction of

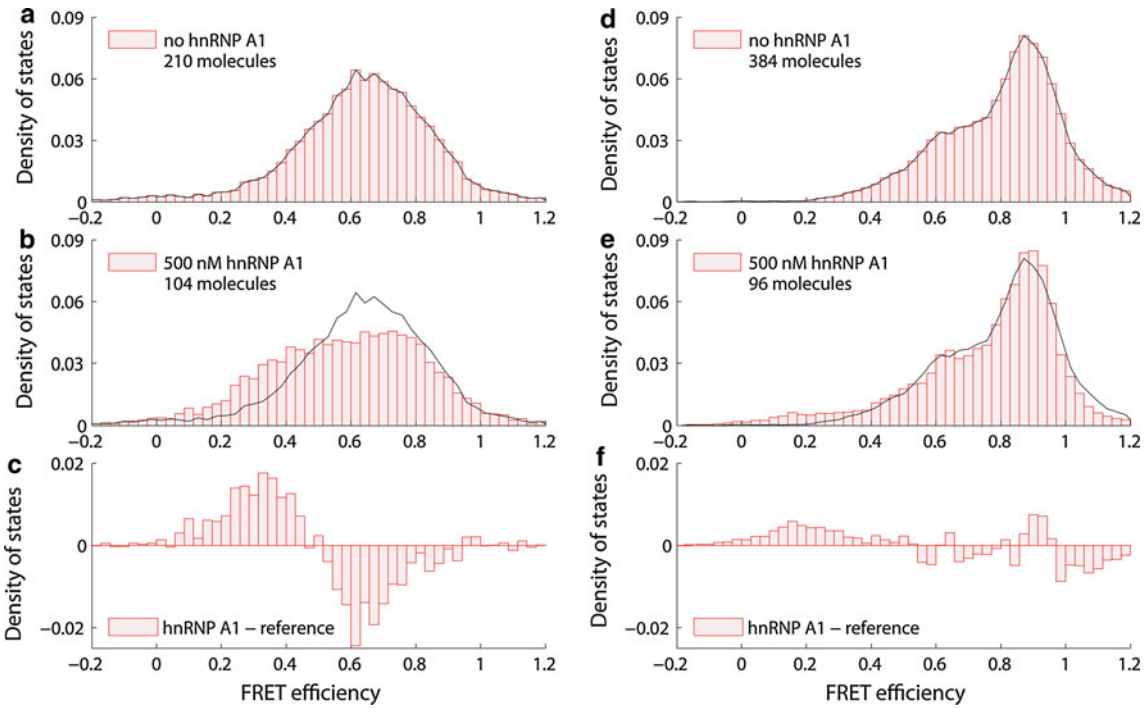

Fig. 3 Effect of the hnRNP A1 protein on the DNA conformations for Tel_I_II (**a**, **b**, **c**) and for Tel_IV_V (**d**, **e**, **f**). The data show single molecule FRET efficiency histograms based on data points from measured single molecule FRET efficiency time traces (density of states as a function of FRET efficiency) for samples containing DNA only (**a**, **d**) and DNA and 500 nM hnRNP A1 (**b**, **e**). The change in the FRET efficiency histogram upon protein addition is plotted in **c**, **f**. Since the different FRET efficiency histograms do not contain the same number of measurements, the data are plotted with the total density of states normalized to one and with the same number of bins for all graphs

possible dimers, which is less than 50%. The observed shift from high to low FRET efficiency in the single molecule measurements upon protein binding is also observed from data where all possible dimer contributions have been removed (data not shown). In addition, we did not observe any increase in the number of possible dimer molecules in the presence of hnRNP A, although dimer molecules have been previously reported to form for the DNA hnRNP A1 complex (Ding et al. 1999). It thus appears that only about 5–13% of the G-quadruplex monomers display a change in conformation to a low FRET efficiency state in the presence of hnRNP A1.

Discussion

The effect of hnRNP A1 binding to telomere DNA constructs was studied by means of a combination of biochemical and biophysical techniques. Importantly, samples were prepared and incubated in similar ways for the gel mobility shift, ensemble FRET, and single molecule FRET assays and are therefore directly comparable.

Specific binding of hnRNP A1 to the telomeric repeat has been observed in several studies (Dallaire et al. 2000; Zhang et al. 2006), and it is reported that a telomeric repeat with a protruding 3′ end binds better than the similar repeat with a protruding 5′ end (Dallaire et al. 2000). This finding is in good accordance with our gel assays where the affinity for the 3′ end overhang of Tel_IV_V was shown to be higher than for the 5′ end overhang of Tel_I_II. The hnRNP A1 binding affinity to Tel_I_II and Tel_IV_V is relatively good as observed in Fig. 2. This is in contrast to our observations from the single molecule FRET experiments (Fig. 3), especially for Tel_IV_V, where we estimated that ∼13% of the G-quadruplex population undergoes a change to a low FRET efficiency state for the Tel_I_II construct and ∼5% for Tel_IV_V. Based on this observation and the position of our fluorophores along the DNA oligos, we suggest that only a fraction of the protein-bound DNA monomer complexes have a truly open conformation. This conformation is most likely different from the one observed in Fig. 1b as the salt concentration in the two buffers is not the same (Lee et al. 2008). In the majority of the complexes, the terminal of the protruding single-stranded DNA end in the protein-DNA complex is as close to the double-stranded DNA region as in a G-quadruplex conformation.

The crystal structure of hnRNPA1 in complex with a short DNA fragment shows that the hnRNP A1 protein recognizes the TTAGG and TAGG repeat via the two

binding sites RRM1 and RRM2 (Ding et al. 1999). This study also showed that the orientation of the protein with respect to the DNA is important: the RRM1 binds preferentially to the 5′ end of the oligo. Figure 4a, b presents the putative arrangements of hnRNP A1 on the Tel_I_II and Tel_IV_V DNA constructs. Both DNA constructs have three full binding sites available.

In the crystal structure, the protein and DNA are forming dimer complexes consisting of two DNA strands, each containing two TTAGGG repeats and two hnRNP A1 proteins. Moreover, other reports indicate that a complex consisting of the UP1 region of hnRNP A1 and a DNA with TTAGGG also form dimers in solution (Myers et al. 2003; Zhang et al. 2006), whereas dimer formation was not observed in studies using intact hnRNP A1 or UP1 (Dallaire et al. 2000). A subpopulation of DNA dimers may be present in our experiments in the absence and presence of hnRNP A1. However, our single molecule FRET analysis shows that the change in DNA conformation from high to low FRET efficiency in the presence of hnRNP A1 is still present when all possible dimer contributions are removed (data not shown).

The crystal structure of the DNA-protein complex shows that the two DNA strands that form dimers are in an open unfolded conformation (Ding et al. 1999), as schematically depicted in Fig. 4c. This complex could be present in our measurements and would appear as a high FRET efficiency state because the acceptor fluorophore in one DNA molecule would come in close proximity to the donor fluorophore in the other DNA molecule. It is, however, not easily distinguishable from a dimer DNA G-quadruplex complex that could also display high FRET efficiency for the same reason. No significant increase in the high FRET efficiency state was observed after hnRNP A1 incubation, which implies that protein binding does not affect the monomer to dimer distribution. These considerations imply that at least 50% of the observed hnRNP A1-DNA complexes consist of one telomeric DNA overhang and one or several hnRNP A1 proteins.

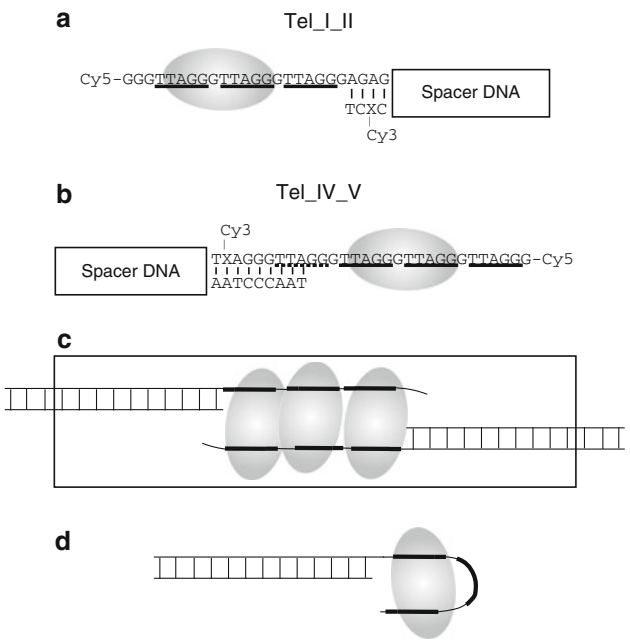

Fig. 4 **a** and **b** Putative models for binding of hnRNP A1 to Tel_I_II or Tel_IV_V. The TTAGG telomere repeat sequences are *underlined*. **a** Tel_I_II with the three expected binding domains available for hnRNPA1 binding. **b** Tel_IV_V with three full binding sites available and the possibility of a fourth one available though duplex breathing (*underlined with dashes*). The potential locations of hnRNP A1 on the DNA constructs are shown schematically. **c** and **d** Structural models of the DNA-protein complexes for DNA dimers (**c**) according to Ding et al. (1999) and for monomers (**d**)

The hnRNP A1 binding efficiency extracted from our gel mobility shift assay is high compared to the number of monomer DNA molecules that have undergone a change of configuration in our FRET assays, even when taking potential dimers into account. To accommodate the two or multiple binding sites for proteins, the monomeric telomeric DNA overhang has to adapt its conformation, and a possible conformation of this complex is shown in Fig. 4d, where we assume that both protein binding sites are active. The relatively high FRET efficiency in the bound state suggests that the DNA-protein complex is in a conformation where the end of the telomeric DNA overhang is rather close to the double-stranded part of the DNA and not much farther away than if the overhang is in a folded G-quadruplex conformation. This finding does not necessarily imply that the G-quadruplex structure is conserved upon protein binding, and unfolding of the G-quadruplex upon UP1 binding has been reported in a number of studies (Fukuda et al. 2002; Myers et al. 2003). We show here that a large fraction of telomeric DNA overhang is not in a completely unfolded state in the monomeric DNA-protein complex as was observed to be the case for telomeric DNA dimers in crystals (Ding et al. 1999).

The family of hnRNP proteins is one of the major G-rich strand telomere binding proteins in nuclear extracts (Ishikawa et al. 1993; Huang et al. 2008). Several reports indicate that hnRNP A1 plays a role in telomere maintenance and telomere length regulation (LaBranche et al. 1998; Dallaire et al. 2000; Zhang et al. 2006). Indeed, hnRNP A1 has been found to protect telomeric DNA against nucleases and to affect the synthesis of telomeric repeats. The unfolding of the G-quadruplex has been suggested to play a role in the latter (Zhang et al. 2006). Here, we report that the telomeric DNA monomer overhang has a rather compact conformation also in the DNA-protein complex. This observation is consistent with the protective role of telomere degradation proposed for hnRNP A1 and may impose limitations as to how accessible telomeric DNA is to enzymes.

In summary, we find that hnRNP A1 binds efficiently to a single-stranded G-quadruplex telomere. Single molecule FRET microscopy measurements reveal that the telomere in complex with one or several hnRNP A1 proteins predominantly has a rather compact configuration. Our observations imply that hnRNP A1 binding may limit the telomere DNA accessibility and are consistent with the protective role suggested for hnRNP A1.

Acknowledgments We would like to acknowledge financial support from the Lundbeck Foundation, the Danish Natural Science Research Council, and the Carlsberg Foundation. We are indepted to Thomas Schmidt and Jesper Donsmark for sharing with us some of their Matlab programs for data analysis.

References

Ambrus A, Chen D et al (2006) Human telomeric sequence forms a hybrid-type intramolecular G-quadruplex structure with mixed parallel/antiparallel strands in potassium solution. Nucleic Acids Res 34(9):2723–2735

Blackburn EH (2001) Switching and signaling at the telomere. Cell 106(6):661–673

Clegg RM (1992) Fluorescence resonance energy transfer and nucleic acids. Methods Enzymol 211:353–388

Cognet L, Harms GS et al (2000) Simultaneous dual-color and dual-polarization imaging of single molecules. Appl Phys Lett 77:4052–4054

Dallaire F, Dupuis S et al (2000) Heterogeneous nuclear ribonucleoprotein A1 and UP1 protect mammalian telomeric repeats and modulate telomere replication in vitro. J Biol Chem 275(19):14509–14516

Ding JZ, Hayashi MK et al (1999) Crystal structure of the two-RRM domain of hnRNP A1 (UP1) complexed with single-stranded telomeric DNA. Genes Dev 13(9):1102–1115

Fiset S, Chabot B (2001) HnRNP A1 may interact simultaneously with telomeric DNA and the human telomerase RNA in vitro. Nucleic Acids Res 29(11):2268–2275

Ford LP, Wright WE et al (2002) A model for heterogeneous nuclear ribonucleoproteins in telomere and telomerase regulation. Oncogene 21(4):580–583

Fukuda H, Katahira M et al (2002) Unfolding of quadruplex structure in the G-rich strand of the minisatellite repeat by the binding protein UP1. Proc Natl Acad Sci USA 99(20):12685–12690

Ha T (2001) Single-molecule fluorescence resonance energy transfer. Methods 25(1):78–86

Heyes CD, Kobitski AY et al (2004) Biocompatible surfaces for specific tethering of individual protein molecules. J Phys Chem B 108(35):13387–13394

Huang PR, Tsai ST et al (2008) Heterogeneous nuclear ribonucleoprotein A3 binds single-stranded telomeric DNA and inhibits telomerase extension in vitro. Biochim Biophys Acta Mol Cell Res 1783:193–202

Ishikawa F, Matunis MJ et al (1993) Nuclear proteins that bind the premessenger RNA 3′ splice-site sequence R(Uuag/G) and the human telomeric DNA-sequence D(Ttaggg)N. Mol Cell Biol 13(7):4301–4310

Kankia BI, Marky LA (2001) Folding of the thrombin aptamer into a G-quadruplex with Sr2 + : stability, heat, and hydration. J Am Chem Soc 123(44):10799–10804

LaBranche H, Dupuis S et al (1998) Telomere elongation by hnRNP A1 and a derivative that interacts with telomeric repeats and telomerase. Nat Genet 19(2):199–202

Lakowicz JR (2006) Principles of fluorescence spectroscopy. Academic/Plenum, NY

Lee NK, Kapanidis AN et al (2005a) Accurate FRET measurements within single diffusing biomolecules using alternating-laser excitation. Biophys J 88(4):2939–2953

Lee JY, Okumus B et al (2005b) Extreme conformational diversity in human telomeric DNA. Proc Natl Acad Sci USA 102(52):18938–18943

Lee JY, Yoon JM et al (2008) Structural diversity and extreme stability of unimolecular Oxytricha nova telomeric G-quadruplex. Biochemistry 47(11):3389–3396

Li J, Correia JJ et al (2005) Not so crystal clear: the structure of the human telomere G-quadruplex in solution differs from that present in a crystal. Nucleic Acids Res 33(14):4649–4659

Luu KN, Phan AT et al (2006) Structure of the human telomere in K+ solution: an intramolecular (3 + 1) G-quadruplex scaffold. J Am Chem Soc 128(30):9963–9970

Myers JC, Moore SA et al (2003) Structure-based incorporation of 6-methyl-8-(2-deoxy-beta-ribofuranosyl)isoxanthopteridine into the human telomeric repeat DNA as a probe for UP1 binding and destabilization of G-tetrad structures. J Biol Chem 278(43):42300–42306

Paeschke K, Simonsson T et al (2005) Telomere end-binding proteins control the formation of G-quadruplex DNA structures in vivo. Nat Struct Mol Biol 12(10):847–854

Patry C, Bouchard L et al (2003) Small interfering RNA-mediated reduction in heterogeneous nuclear ribonucleoparticule A1/A2 proteins induces apoptosis in human cancer cells but not in normal mortal cell lines. Cancer Res 63(22):7679–7688

Roy R, Hohng S et al (2008) A practical guide to single-molecule FRET. Nat Meth 5(6):507–516

Schmidt T, Schuetz GJ et al (1995) Characterization of photophysics and mobility of single molecules in a fluid lipid membrane. J Phys Chem 99(49):17662–17668

Tange TØ, Damgaard CK, Guth S, Valcarcel J, Kjems J (2001) The hnRNP A1 protein regulates HIV-1 tat/rev intron splicing via a novel intronic silencer element. EMBO J 20:5748–5758

Wang Y, Patel DJ (1993) Solution structure of the human telomeric repeat D[Ag(3)(T(2)Ag(3))3] G-tetraplex. Structure 1(4):263–282

Xu Y, Noguchi Y et al (2006) The new models of the human telomere d[AGGG(TTAGGG)(3)] in K+ solution. Bioorg Med Chem 14(16):5584–5591

Yildiz A, Forkey JN et al (2003) Myosin V walks hand-over-hand: single fluorophore imaging with 1.5-nm localization. Science 300(5628):2061–2065

Ying LM, Green JJ et al (2003) Studies on the structure and dynamics of the human telomeric G quadruplex by single-molecule fluorescence resonance energy transfer. Proc Natl Acad Sci USA 100(25):14629–14634

Zahler AM, Williamson JR et al (1991) Inhibition of telomerase by G-quartet DNA structures. Nature 350(6320):718–720

Zhang QS, Manche L et al (2006) hnRNP A1 associates with telomere ends and stimulates telomerase activity. RNA 12(6):1116–1128